CHARGE DISTRIBUTION AND CONFORMATIONS OF WEAK POLYELECTROLYTE CHAINS IN POOR SOLVENTS

Peter KOŠOVAN[1], Zuzana LIMPOUCHOVÁ[2] and Karel PROCHÁZKA[3,*]

Department of Physical and Macromolecular Chemistry, Faculty of Science, Charles University, Hlavova 8, 128 43 Prague, Czech Republic; e-mail: [1] kosovan@vivien.natur.cuni.cz, [2] zl@vivien.natur.cuni.cz, [3] prochaz@vivien.natur.cuni.cz

Received December 20, 2007
Accepted February 12, 2008
Published online April 25, 2008

Dedicated to Professor William R. Smith on the occasion of his 65th birthday.

In this work we study the effect of mobility of charges in annealed polyelectrolytes on their conformational behavior in poor solvents. A combination of molecular dynamics and Monte Carlo simulation techniques was used to take the dissociation into account. We investigated the relation between the conformation of the polyelectrolyte and the distribution of charges along the chain. The results suggest that in sufficiently poor solvents the local degree of charging differs significantly from the average. When a pearl-necklace conformation is formed, the degree of charging of the pearls is significantly lower than that of the strings. The redistribution of charges stabilizes the pearl-necklace conformation and enables the formation of asymmetric conformations with a single pearl at one chain end and a string at the other end.

Keywords: Annealed polyelectrolytes; Molecular dynamics; Monte Carlo; Simulation; Polymers; Pearl-necklace; Poor solvent; Conformation.

Polyelectrolytes (PE) are polymers containing ionizable groups that can dissociate in polar solvents, leaving electric charges on the chain and producing small mobile counterions that can escape into the bulk solution. Due to electrostatic interactions, the behavior of polyelectrolyte solutions is very rich and differs in many respects from that of neutral polymers.

Polyelectrolytes play a very important role in biological processes and in various technical and technological applications, e.g., microcapsules formed by layer-by-layer deposition of polyanions and polycations on the surface of colloidal microspheres may be used as microcontainers for targeted drug delivery and other purposes[1]. Typical examples of biologically

Collect. Czech. Chem. Commun. 2008, Vol. 73, No. 4, pp. 439–458

doi:10.1135/cccc20080439

important polyelectrolytes are nucleic acids and proteins. Their vital role in biochemical processes does not need to be stressed.

With respect to the dissociation behavior, chemists classify polyelectrolytes into two classes: strong and weak. In strong polyelectrolytes, the positions and the number of charged groups on the chain are determined by synthesis. Once the polymer is synthesized, they are independent of external conditions. The charge distribution on the strong polyelectrolyte is "quenched" and therefore the term "quenched polyelectrolyte" is used by theoreticians. In weak polyelectrolytes, the dissociation depends on pH, ionic strength and other parameters of the system. Under equilibrium conditions, the pairs of opposite charges (one remaining on the chain and the other escaping into the bulk) appear and disappear in different positions on the chain via reversible dissociation/association processes with a fairly high frequency. Hence the distribution of charges is an "annealed variable". This is why weak polyelectrolytes are also called "annealed polyelectrolytes".

Due to high importance of polyelectrolytes, their solutions and melts have been studied for a long time by a number of teams of experimentalists, theoreticians and also by computer simulations[1–3]. The number of published studies is so vast that it is futile to give all relevant references. In the following text, we include only references to several review articles and to the most important seminal studies relevant for the studied topic.

It was realized relatively early that a sparsely ionized polyelectrolyte chain in a poor solvent will form a compact globular conformation while the conformation of the same kind of polymer which is highly ionized will be much more expanded. Hence the effective solvent quality for a polyelectrolyte is not only a function of the type of polymer, solvent and temperature but also of the degree of ionization. A solvent which is poor for the polymer when it is almost neutral may be a good solvent for the same polymer when it is charged. The up-to-date understanding of the behavior of polyelectrolytes has been achieved by several approaches. Besides a number of experimental studies, the current understanding of solution behavior of polyelectrolytes stems from various theoretical approaches, namely the solution of integral equations, e.g., Polymer-Reference-Interaction-Site model, PRISM, with the Reference-Laria-Wu-Chandler closure[4], perturbation theories[5] and computer simulations where, e.g., Micka, Kremer, Stevens et al.[6–11] contributed to recent advances in this field.

Because we are studying the behavior of annealed PEs in poor solvents, we focus our attention on poor solvent behavior. We begin with the description of quenched PEs to show some common features and then extend

the description to weak PEs. The first theoretical attempt to treat the quenched polyelectrolyte chain in poor solvent was made by Khokhlov[12]. He has shown that with increasing degree of charging the spherically symmetrical globular conformation would deform to a prolate ellipsoid (almost a cylinder).

Afterwards, the so-called pearl-necklace model appeared. It was first suggested by Ghiggino et al.[13] on the basis of indirect fluorescence study of the behavior of poly(methacrylic acid), even though this paper is almost unknown. Kantor and Kardar in their theoretical paper[14] explained that the same physical arguments as used by Rayleigh in 1882 when he explained the instability of charged oil droplets[15] can be used to describe the conformational change in a hydrophobic polyelectrolyte. The repulsion of electric charges in the droplet tends to expand it, which is counteracted by the tendency to lower the surface energy by contracting the droplet. When a critical charge is reached, the droplet becomes unstable and splits into two smaller droplets which can then move away from each other and thus lower the electrostatic energy. Analogous arguments explain the formation of "pearls" on the PE chain. In poor solvents, an attempt to minimize the number of unfavourable interactions between the polymer segments and solvent molecules leads to a compact globular conformation with minimized surface area. When the charge in the globule is such that the Rayleigh instability condition is fulfilled, it splits into two smaller globules. Because of chain connectivity, the daughter globules (pearls) are kept at a certain distance by a stretched part of the chain and cannot separate from each other. More detailed (and at present generally accepted) description was provided one year later by the model of Dobrynin, Rubinstein and Obukhov[16]. It predicts a cascade of transitions with integer numbers of pearls. The above hypothesis was confirmed both by Monte Carlo (MC) and molecular dynamics (MD) simulations[9] and, at present, it is a generally accepted scheme of behavior of quenched PE chains.

In annealed polyelectrolytes the situation is more complex. The probability of dissociation of a particular ionizable group depends, among other factors, on its distance from the nearest already ionized group. Hence the distribution of charges may change in a cooperative manner with a change in conformation. A simultaneous ionization of two close groups is unfavourable (e.g., the dissociation of the second COOH group in oxalic acid is strongly hindered and the ratio of the second-to-first step dissociation constants, K_2/K_1 is around 10^{-3} (ref.[17]). In the case of an annealed flexible PE this means that the charges prefer such positions on the chain that their mutual interaction energy is minimized, which is related to the conforma-

tion of the polymer. Therefore it is not surprising that both theoretical and computer studies predict behavior which differs from that of quenched PEs.

It was predicted theoretically by Raphael and Joanny[18] that with a change in pH a weak polyelectrolyte in poor solvent should undergo a first-order transition from a highly charged expanded conformation to a collapsed conformation with very low ionization. Recent MC simulations in semi-grand canonical ensemble at a fixed chemical potential of the charges show some controversy with respect to these predictions. Some authors claim that the conformational transition proceeds via the pearl-necklace conformations[19] even in very poor solvents while others[20] claim that deep in a poor solvent the transition is first-order as predicted by Raphael and Joanny and only close-to-theta solvent the transition may proceed via the necklace of pearls. Also Leibler et al. recently argued that the plateau on the titration curves does not have to be related to sharp conformational transitions[21].

In this paper, we present we present a combination of molecular dynamics and MC simulation techniques which accounts for the mobility of charges. We focus our attention on the relation between the distribution of charges along the chain of an annealed polyelectrolyte and its conformation. This issue has not been addressed in any of the above-mentioned studies. A theoretical description of the distribution of charges on a weak polyelectrolyte in good solvent[22] shows that except for the chain ends the local degree of charging does not significantly deviate from the average value. This has only a marginal effect on the polymer conformation. To our best knowledge no such study (simulation or theory) exists for the poor solvent case which, according to our results, exhibits certain interesting features.

MODEL AND SIMULATION TECHNIQUE

Simulation Technique

We are using MD simulations with the Langevin termostat[6]. It is based on the solution of classical Newtonian equations of motion modified by two additional forces

$$m\frac{\mathrm{d}^2\boldsymbol{r}_i}{\mathrm{d}t^2} = -\nabla\sum_{j\neq i}U(r_{ij}) + \boldsymbol{F}_i^{\mathrm{D}} + \boldsymbol{F}_i^{\mathrm{R}} \qquad (1)$$

where $\boldsymbol{r}_i$ is the position vector of i-th particle, m is its mass, t is time and $U(r_{ij})$ the interaction potential. The dissipative force $\boldsymbol{F}_i^{\mathrm{D}}$ and the random force $\boldsymbol{F}_i^{\mathrm{R}}$ emulate the collisions with solvent molecules which are not included explicitly in the model. These forces are defined by the following relations

$$\boldsymbol{F}_i^{\mathrm{D}} = -m\Gamma \frac{\mathrm{d}\boldsymbol{r}_i}{\mathrm{d}t} \tag{2}$$

$$\langle \boldsymbol{F}_i^{\mathrm{R}}(t) \cdot \boldsymbol{F}_i^{\mathrm{R}}(t') \rangle = 6\Gamma k_{\mathrm{B}} T m \delta_{ij} \delta(t - t') \tag{3}$$

$$\langle \boldsymbol{F}_i^{\mathrm{R}}(t) \rangle = 0 \tag{4}$$

where k_{B} is the Boltzmann constant and Γ is the friction constant related to solvent viscosity.

The use of the implicit solvent prevents us from obtaining all details on the behavior, but it significantly reduces the number of degrees of freedom of the simulated system. Thus much longer simulation times are accessible in comparison with models which use an explicit solvent.

The simulations were performed using the Espresso software package[23,24] which has been designed specially for simulations of polyelectrolyte systems in implicit solvents with explicit counterions and electrostatic interactions.

Polymer Model

The polymer is represented as a chain of beads connected by elastic springs. One bead of the model may represent one or more monomer units depending on how the model is mapped onto a real polymer. The polymer is modeled as a freely jointed chain, i.e., there are no restrictions on bond angles. The model is schematically depicted in Fig. 1. The simulation is performed in the dilute solution limit and the solution contains no added salt. The particle density is $10^{-5}\,\sigma_{\mathrm{L-J}}^{-1}$ ($\sigma_{\mathrm{L-J}}$ is the reduced unit of length, for more details see the next Section), i.e., the dimension of the cubic simulation box is significantly larger than the end-to-end distance of the polymer. This assures that the molecule does not interact with itself as an artifact of periodic boundary conditions. How much exactly the box length is larger than the end-to-end distance depends on the conformation but even for the

most expanded conformations the difference is about 50%, which is just enough.

The van der Waals interactions between individual monomer units are modeled by the Lennard–Jones potential (L–J) with a finite cutoff and an appropriate shift

$$U_{\mathrm{L-J}} = \begin{cases} 4\epsilon_{\mathrm{L-J}}\left[\left(\frac{\sigma_{\mathrm{L-J}}}{r}\right)^{12} - \left(\frac{\sigma_{\mathrm{L-J}}}{r}\right)^{6} + c(R_{\mathrm{c}})\right] & \text{for } r \le R_{\mathrm{c}} \\ 0 & \text{for } r \ge R_{\mathrm{c}} \end{cases} \qquad (5)$$

where $c(R_{\mathrm{c}}) = (\sigma_{\mathrm{L-J}}/R_{\mathrm{c}})^{12} - (\sigma_{\mathrm{L-J}}/R_{\mathrm{c}})^{6}$ and $R_{\mathrm{c}} = 2.5\,\sigma_{\mathrm{L-J}}$ is the interaction cutoff radius. In most synthetic polymers, the monomer units are hydrophobic. Their interaction with the solvent is unfavorable and they prefer to cluster and remain close to each other. In implicit solvent models, this effect is treated as an effective attraction between the monomer units. The hydrophobicity of the polymer is then controlled by the depth of the potential minimum, $\epsilon_{\mathrm{L-J}}$. The higher the value of $\epsilon_{\mathrm{L-J}}$, the more hydrophobic the polymer, i.e., the worse the solvent quality. The size of the monomer units is controlled by the $\sigma_{\mathrm{L-J}}$ parameter. The actual values of the interaction parameters that we have used are discussed in the next Section.

The excluded volume of counterions is modeled by the purely repulsive part of the Lennard–Jones potential

$$U'_{\mathrm{L-J}} = \begin{cases} 4\epsilon'_{\mathrm{L-J}}\left[\left(\frac{\sigma'_{\mathrm{L-J}}}{r}\right)^{12} - \left(\frac{\sigma'_{\mathrm{L-J}}}{r}\right)^{6}\right] + \epsilon'_{\mathrm{L-J}} & \text{for } r \le R'_{\mathrm{c}} \\ 0 & \text{for } r \ge R'_{\mathrm{c}} \end{cases} . \qquad (6)$$

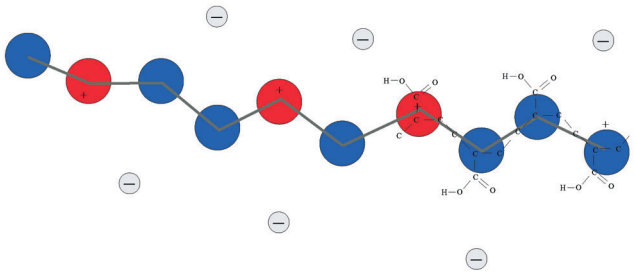

FIG. 1
Schematic illustration of the polymer model. Blue spheres represent uncharged monomer units, red spheres the charged ones and grey the counterions

"Chemical bonds", i.e., bonds between beads forming the polymer backbone are described by the finite-extension nonlinear elastic (FENE) potential

$$U_{\mathrm{FENE}} = -\frac{1}{2} K_{\mathrm{FENE}} R_{\mathrm{FENE}}^2 \ln\left(1 - \left(\frac{r}{R_{\mathrm{FENE}}}\right)^2\right). \qquad (7)$$

The long-range nature of the electrostatic Coulomb potential precludes the use of a finite cutoff as it was done in the case of the L–J potential. The elec-

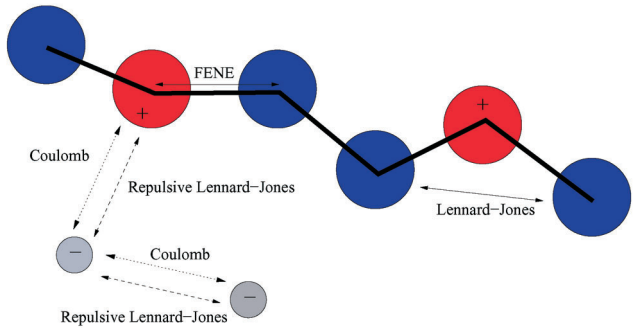

FIG. 2
Schematic illustration of interaction types used in the polymer model

trostatic interactions are treated using the particle–particle particle–mesh algorithm for the Ewald summation implemented in Espresso[23]. All interactions used in the model are schematically shown in Fig. 2.

Interaction Parameters and Reduced Units

The interaction parameters used in this work are summarized in Table I. We use $\sigma_{\mathrm{L-J}}$ as our unit of length, setting $\sigma_{\mathrm{L-J}} = 1.0$ for all particles. Mapping the model onto the real system so that one bead corresponds to one monomer unit, we get $\sigma_{\mathrm{L-J}} \approx 2.5$ Å. Another parameter with the dimension of length is the Bjerrum length, λ_{B}, defined as

$$\lambda_{\mathrm{B}} = \frac{e^2}{4\pi\varepsilon_0\varepsilon_r k_{\mathrm{B}} T} \qquad (8)$$

where ε_r is the relative permittivity of the bulk system and e is the elementary charge. Having σ_{L-J} 2.5 Å, we set $\lambda_B = 2.85\,\sigma_{L-J} \approx 7.1$ Å, which corresponds to aqueous solutions at room temperature. For the FENE potential we set $K_{FENE} = 7.0$ and $R_{FENE} = 2.0$. These values, combined with the L–J potential, assure the average bond length to be about $1.0\,\sigma_{L-J}$. We set the friction constant $\Gamma = 1.0\,\tau^{-1}$, where $\tau = \sigma_{L-J}\sqrt{m / k_B T}$ is the standard L–J unit of time. The integration of the equations of motion is then performed with time step $\Delta t = 0.0125\tau$ and the whole simulation lasts typically $3 \times 10^5\,\tau$. Taking $M \approx 100$ g/mol as a typical molar mass of a monomer unit, we get $\tau \approx 1.5$ ps.

For the short-range interaction of counterions (U'_{L-J}, Eq. (*6*)) we set $\epsilon'_{L-J} = 1.0$. The exact value of this parameter is of little significance. This can be shown by calculating the second virial coefficient of particles interacting with this type of potential which depends only weakly on the actual value of ϵ'_{L-J}. The size of the counterions is set to be equal to that of the monomer units, $\sigma'_{L-J} = 1.0\,\sigma_{L-J}$. In the context of implicit solvent model this can be viewed as modeling the counterion together with its first hydration shell[7].

The ϵ_{L-J} parameters of individual monomer units are of much greater significance because they determine the solvent quality for the polymer. As a reference, we take the Θ state of a neutral polymer. For the bead-spring polymer model interacting via the L–J potential with the same parameters as we use here, Micka, Holm and Kremer[10] have determined that $\epsilon_{L-J} =$

TABLE I
Parameters of the simulated polymers

Parameter	Value	Comment
Chain length	512 segments	
Dissociation rate constant	$k = 10^7$ s^{-1}	corresponds to $K_A = 10^{-3}$
Degree of dissociation	$\alpha = 0.12$–0.33	
Bjerrum length	$\lambda_B = 2.85\sigma_{L-J}$	aqueous solution
Hydrophobicity	$\varepsilon_{L-J} = 1.00$ $\varepsilon_{L-J} = 0.60$	poor solvent moderately poor solvent

0.34 ± 0.02 corresponds to the Θ state. In our simulations we use ϵ_{L-J} = 0.6 and 1.0. Both these values correspond to the hydrophobic regime but the lower value gives a less hydrophobic polymer. Hence, in this paper we refer to the polymer with ϵ_{L-J} = 0.6 as moderately hydrophobic and to the one with ϵ_{L-J} = 1.0 as the more hydrophobic or strongly hydrophobic.

The Model of Dissociation

We propose a simple model of dissociation which accounts for the mobility of charges along the weak PE chain. We assume that a single dissociation event is very fast compared to both the time between two such events and a typical integration step of our MD simulation. Hence we choose a random charged unit on the polymer chain and change it to uncharged. To keep the whole system electrically neutral, we assume that at the same time an association takes place in another part of the polymer chain. Effectively, this means that we move the charge from one place to another, imposing a constraint of a fixed degree of dissociation of the PE. In the limit of infinitely long chain, this assumption is correct but it may introduce some artifacts when applied to a PE of finite length. This issue will be discussed later.

We assume that the dissociation occurs as a first-order process with rate constant *k*. This assumption is reasonable for a time interval in which the probability of dissociation is relatively small. In this case, the probability

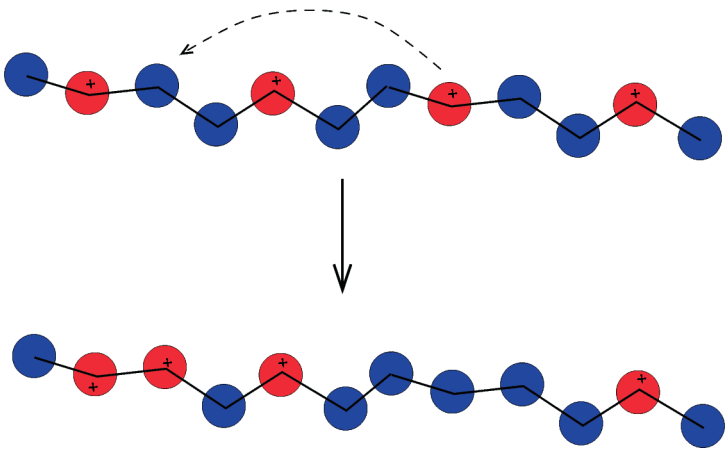

FIG. 3
Schematic illustration of the charge move MC simulation step. Blue spheres represent uncharged monomer units, red spheres the charged ones

that a dissociation and a re-association both take place within the same time interval is even smaller and hence the reverse process can be neglected. As follows from the simulation algorithm, the reverse process is not completely ignored because a monomer unit which has lost its charge in one dissociation event can regain the charge when another monomer unit loses it.

When there are n charged monomer units on the chain, the dissociation events should occur with frequency kn. In the simulation it is realized so that with this frequency we randomly choose one charged and one uncharged monomer unit and attempt to move the charge from one to the other (Fig. 3). The attempt is accepted or discarded using the Metropolis criterion[25]: if the energy of the new configuration is lower than the old one, it is accepted; if the energy of the new configuration is higher, then the move is accepted with the probability $p = \exp(-\Delta U/k_B T)$, where ΔU is the difference between the energies of the original and the attempted new configuration. The acceptance ratio is smaller than 1.0 which results in somewhat lower dissociation rates than desired but this is of minor significance since both the rate constants and the time units of the simulation are only estimates of the order of magnitude. Moreover, the rate does not affect the thermodynamic equilibrium, it only affects how quickly the system converges to it. In the simulation, we set the rate constant $k = 10^7$ s^{-1} which is a typical value for a weak acid with $K_A \approx 10^{-3}$ (ref.[26])

Of course, the actual value of the rate significantly influences the dynamics of the system but the dynamics is not the subject of the current study. Yet, the simulation method employed is molecular dynamics and we have to discuss briefly to what extent the results can be influenced by perturbations caused by sudden moves of charges from one position to another and by the rate of this process. If it was a standard MD in the [N, V, E] ensemble, the swapping of charges would have a fatal effect on the integration of the equations of motion. In the Langevin thermostat, however, the random forces dissipate perturbations imposed by the instantaneous changes in the system. For this to be acceptable, the perturbations should not be much larger than $k_B T$. The extent of a possible perturbation that can occur in the system may be estimated by analyzing the effect of moving the charge from a highly charged part of the chain to the uncharged part of the chain. Assuming that in the original position both neighboring units are charged and the charge is moved to a position where there are no charges around, the energy change in the system would be almost $6k_B T$. Yet the effect is clearly overestimated because of the screening effect of the counterions which was not taken into account. Moreover, with our parameter values,

the linear charge density in a part of the chain where several neighboring units are charged just fulfils the condition for counterion condensation. The condensed counterions would compensate the charge even more than the average counterion cloud. Also, the extreme situation when several neighboring units are charged hardly occurs in our simulations as the average degree of charging even for the highly charged parts of the chain is only about 0.3 (see further, Fig. 9). The analysis of the simulation data shows that the energy change caused by a single dissociation event is typically a fraction of kT.

With the friction constant $\Gamma = \tau^{-1}$, the perturbations decay on the time scale of τ. If the dissociations occurred on a time scale comparable to τ, they would be a major problem but since the dissociation rate is slow when compared to τ, the perturbations are dissipated relatively quickly and the system returns to its normal state. However, it has to be kept in mind that the motion of charges distorts time correlations in the studied system in an undefined way and, therefore, it is not possible at present to draw quantitative conclusions on the dynamics of the system.

RESULTS AND DISCUSSION

Simulation Snapshots

We have performed simulations of polyelectrolyte chains composed of 512 segments under poor solvent conditions. We have used two different values of the ϵ_{L-J} parameter which determines the solvent quality for the polymer (Table I). For the purpose of this study, the solvent with $\epsilon_{L-J} = 0.6$ is refered

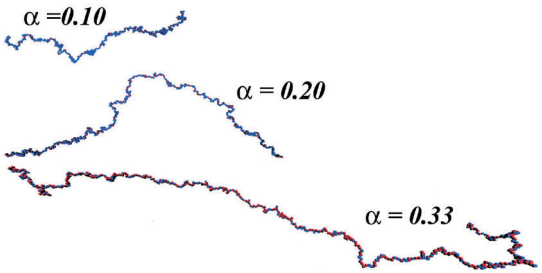

FIG. 4
Simulation snapshots of chain conformations in a moderately poor solvent for three degrees of ionization, α, 0.10, 0.20 and 0.33

to as moderately poor solvent, the one with ϵ_{L-J} = 1.0, is refered to as poor solvent. Simulations in the range of degrees of dissociation, α, 0.10–0.33, have been performed. In experiment, the degree of dissociation is a function of pH. In our simulation we use it as an adjustable parameter and simulate at a constant value of α.

An instructive view (but least exact from the statistical point of view) of the polymer conformations is provided by simulation snapshots. Typical snapshots of a moderately hydrophobic polyelectrolyte are shown in Fig. 4 for three degrees of ionization, α, 0.10, 0.20 and 0.33. In this solvent, the polymer backbone is still fairly soluble and the PE chain is quite stretched. The conformations shown do not significantly differ except for the trivial observation that the elongation increases with the degree of dissociation.

A different picture is obtained for the more hydrophobic polymer. The corresponding typical simulation snapshots are shown in Fig. 5 for the degrees of ionization, α, 0.10, 0.20 and 0.33. At lower degrees of dissociation one or two pearls are formed at the chain ends, at higher degrees of dissociation one and then the other pearls are transformed to a stretched part of the chain. This corresponds to the model of Dobrynin, Rubinstein and Obukhov[16] derived for strong polyelectrolytes.

The formation of the highly asymmetric conformation consisting of a single pearl and a single stretched string at α = 0.20 (Fig. 5) is somewhat unexpected. First we suspected that it could either be a metastable state or a simulation artifact. For this reason we tested several initial configurations and dissociation rates and it showed up that the polymer adopts this type

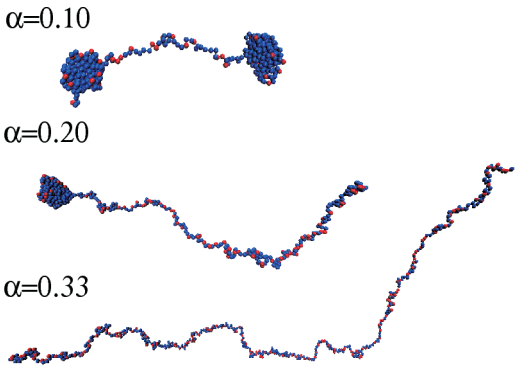

FIG. 5
Simulation snapshots of chain conformations in a bad solvent for three degrees of ionization, α, 0.10, 0.20 and 0.33

of conformation independently of both factors. The formation of the asymmetric conformation can be rationalized by the following arguments: In contrast to quenched polyelectrolytes, the splitting of charged globules is not the only mechanism by which an annealed polyelectrolyte can lower its energy. The existence of compact globules in a quenched polyelectrolyte is hindered by the fact that it results in a high charge density confined in the small volume of the globule. Yet the globules are formed anyway. With mobile charges, further decrease in energy can be gained by transferring a charge from inside the globule to another part of the chain which may have a higher linear charge density but the spatial density may be lower due to the different local conformation. It will be shown in the following text that, indeed, the distribution of charges and local conformation of the chain are correlated.

Charge Distribution and Bond-Angle Cosines

More quantitative information than that provided by the simulation snapshots can be obtained from various functions that characterize the local conformation of the chain and are obtained as an average over a number of sampled conformations.

To make a quantitative analysis of the local polymer conformation, average bond-angle cosines can be used. We define the bond-angle cosine, $\langle\cos(\theta_i)\rangle$, as the scalar product of bond vectors $\vec{r}_i$ (the direction of bond from monomer unit i to $i + 1$) and $\vec{r}_{i+1}$ (from $i + 1$ to $i + 2$) divided by the product of their magnitudes

$$\langle\cos(\theta_i)\rangle = \frac{\langle \vec{r}_i \cdot \vec{r}_{i+1} \rangle}{|\vec{r}_i||\vec{r}_{i+1}|} . \qquad (9)$$

Here the angular brackets denote ensemble averaging. The expected values of the bond-angle cosines for various local conformations are schematically illustrated in Fig. 6. For a monomer unit which is located in the part of the chain that is collapsed, the average bond-angle cosine is expected to be close to zero because the only restriction for the bond angle is the excluded volume of the neighbouring monomer unit which forbids the values of θ close to 180°. On the other hand, if the monomer unit is inside a highly stretched part of the chain, the average bond-angle cosine is close to one. In this case the major restriction to the bond angle comes from the chain stretching which allows only for the values of θ close to zero.

The average bond-angle cosines for the moderately hydrophobic polyelectrolyte exhibit no interesting features, therefore we do not show the plots here. We restrict ourselves to a statement that they are all qualitatively similar to Fig. 7, $\alpha = 0.33$, which is in agreement with the simulation snapshots showing stretched conformations. The average bond-angle cosines for the more hydrophobic polyelectrolyte are plotted in Fig. 7. The data show that some parts of the chains are strongly expanded while other parts are collapsed. Figure 7 shows the formation of two pearls at the chain ends for $\alpha = 0.10$ (the plateaus in the plot) and a stretched central part of the chain (the peak in the plot around $i \approx 250$). For $\alpha = 0.20$ Fig. 7 shows the formation of a single pearl (right part of the plot) at one chain end and a stretched conformation at the other end (left part of the plot). For $\alpha = 0.33$ a stretched conformation along the whole chain can be seen from Fig. 7. This gives a quantitative basis to the preliminary conclusions about the formation of pearls that we have drawn from the simulation snapshots. From the bond-angle cosines it can be seen that it is not only a feature of a single conformation, but it is a general feature of the conformational behavior and that the pearls are well localized.

To analyze the charge distribution along the polymer chain we define the function $P(q,i)$ as a probability that a monomer unit i is charged or not. Taking an average over many conformations, this function gives the average (local) degree of dissociation as a function of the position of the monomer unit in the chain.

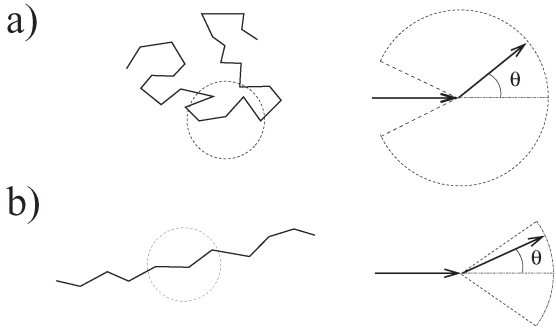

FIG. 6
Schematic illustration of the possible values of bond-angle cosines

In the case of a strong polyelectrolyte, the degrees of ionization of individual monomer units are fixed once the polymer is synthesized. Hence the function $P(q,i)$ is a step function that can have a value of either 0 or 1 for each value of i. On the other hand, in the case of a weak polyelectrolyte, $P(q,i)$ is expected to vary smoothly with i.

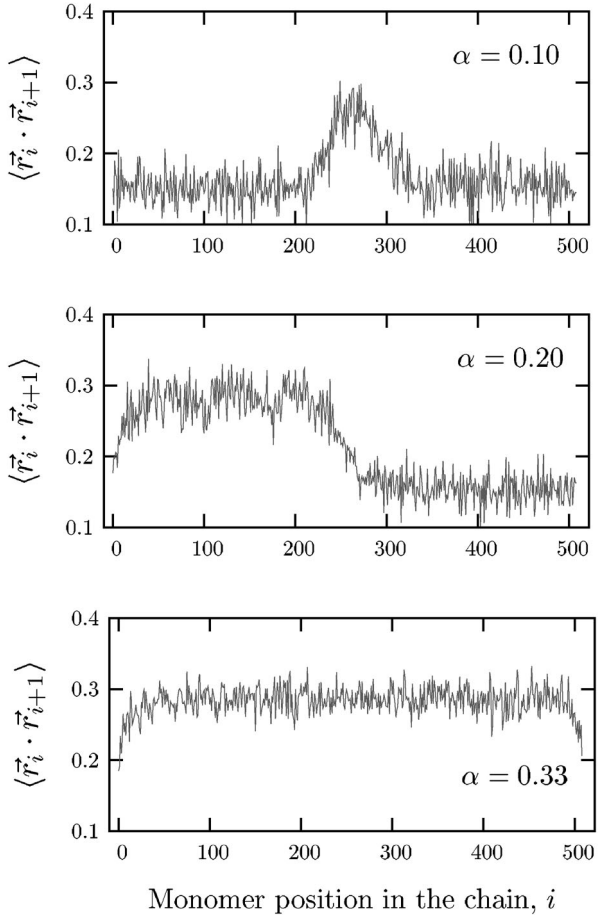

FIG. 7
Average bond-angle cosines as functions of the position of the monomer unit in the polymer chain for the more hydrophobic polymer (ϵ = 1.0)

The function $P(q,i)$ for the moderately hydrophobic polyelectrolyte is shown in Fig. 8 for α = 0.10, 0.20 and 0.33. In all cases, the local degree of dissociation fluctuates around the value of α. It slightly increases towards both ends of the chain which is in agreement with observation of other authors for polyelectrolytes in good solvents[22].

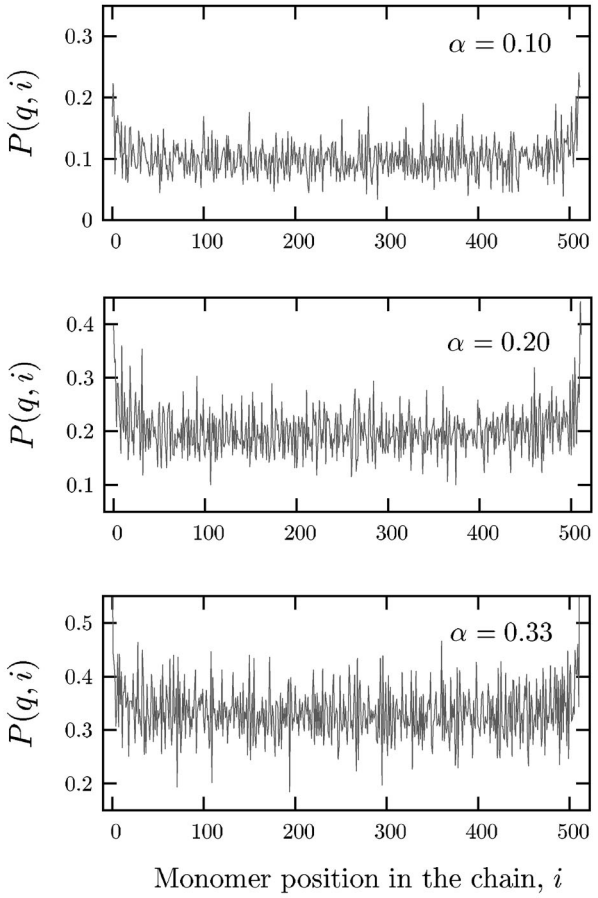

FIG. 8
The probability of charging of individual monomer units, $P(q,i)$, in a moderately poor solvent as a function of their position in the chain, i, for α = 0.1, 0.2 and 0.33

The data are rather noisy, which is due to the high computational demands of the calculations. Each figure represents an average over about 10^3 conformations and typically about 10^2 dissociation events occur between two sampled conformations. The noise could be reduced by prolonging the simulation times but the important features of the graphs are clearly visible anyway. An attempt to make the plots significantly smoother would require unacceptably long simulation times (more than a month of CPU time per simulation).

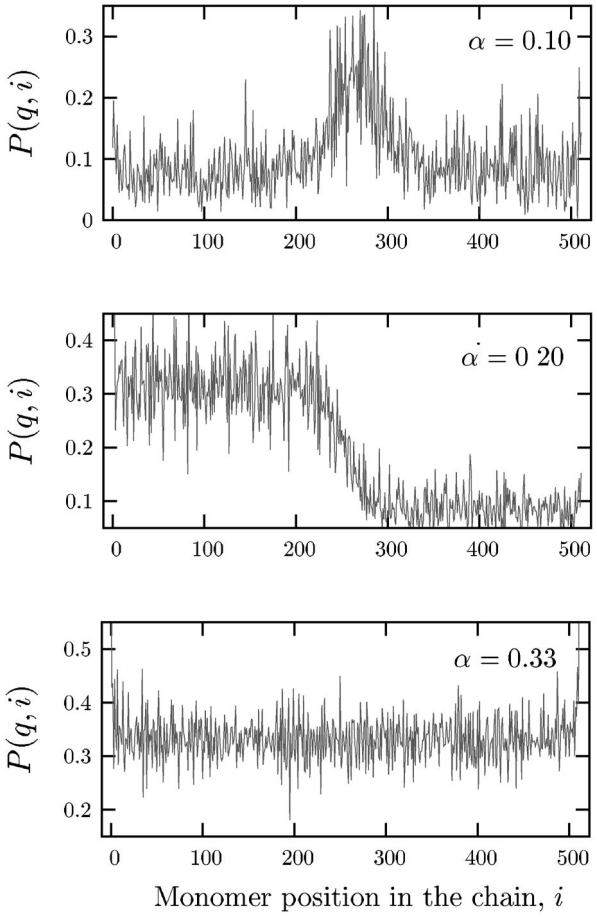

FIG. 9
The probability of charging of individual monomer units, $P(q,i)$, for the more hydrophobic polymer, as a function of their position in the chain, i, for α = 0.1, 0.2 and 0.33

The probability of charging, $P(q,i)$, as a function of monomer position in the chain in the case of the more hydrophobic polyelectrolyte is shown in Fig. 9 for the degrees of dissociation $\alpha = 0.10$, 0.20 and 0.33 respectively. Comparing the data to the corresponding bond-angle cosines shown in Fig. 7, we can correlate the average local degree of dissociation and the local conformation. At $\alpha = 0.10$, the central part of the chain is highly charged while the parts of the chain that are further from the centre carry much less charge. This well compares to Fig. 7 and one can see that the degree of ionization of the stretched part is significantly higher than that of the pearls. The same relation between the conformation and the distribution of charges holds for the case of $\alpha = 0.20$ with the only difference that there is only one pearl at one chain end now. Figure 9 shows no significant differences in the degree of dissociation along the chain for $\alpha = 0.33$, which is in agreement with the fact that no pearls are formed (Fig. 9). We can conclude that when the collapsed domains are formed, the degree of ionization inside the pearls is well below the average value while in the stretched parts of the chain the local degree of ionization is well above the average.

The conformational change and the redistribution of charges are clearly interconnected and proceed in a cooperative manner. As it has been argued earlier using qualitative arguments, this is a consequence of the mobility of charges in a weak polyelectrolyte which serves as an additional mechanism of lowering the interaction energy. Earlier simulations on quenched polyelectrolytes in poor solvents[8,9] claim that although the pearls exist and can be observed in simulation snapshots, they fluctuate a lot and hence might be difficult to detect experimentally. Although the dynamics of our model is distorted and hence we cannot obtain direct information on the dynamics of the system, we can draw a qualitative conclusion that the pearls formed by a weak polyelectrolyte should be dynamically more stable since the mobility of charges provides additional stabilization.

Possible Artifacts of the Model

Having discussed how the mobility of charges affects the conformations and properties of polyelectrolytes, it is necessary to discuss possible artifacts of the model. In our simulation, we use the degree of dissociation as a fixed parameter which can be continuously varied. The theoretical predictions of Raphael and Joanny[18] as well as some Monte Carlo simulations[20] suggest that for polymers that are more hydrophobic than a certain threshold a certain region of degrees of dissociation is forbidden and a first-order transition from an uncharged and collapsed to a fully or partly dissociated and

expanded conformation occurs. To make a reasonable comparison with the semi-grand canonical MC simulations, a more sophisticated MD model is necessary, which would explicitly treat the dissociation into the bulk solvent. Development of such model is currently in progress.

Nevertheless, current simulation results show that the mobility of charges by itself causes the conformational behavior of annealed PEs to be different from that of systems with a fixed distribution of charges. Even though the study does not yet allow us to draw definite conclusions on the conformational transition, the results show an additional mechanism of charge balancing between collapsed and elongated parts of annealed PE chains which stabilizes the pearls at fixed positions. Thus the conformational change proceeds differently from that in quenched polyelectrolytes.

CONCLUSION

The mobility of charges in a weak polyelectrolyte has, under certain conditions, a significant effect on its conformation. If the solvent is only moderately poor and the chain is in an expanded conformation, the local degree of charging shows only small deviations from the average one. In poorer solvents where collapsed domains are formed, the local degree of charging in the collapsed domains decreases at the expense of increase of the degree of charging of the stretched domains (strings). The redistribution of charges provides an additional mechanism of lowering the energy of the system and stabilizes the pearl-necklace conformation. In a certain range of conditions, this may lead even to asymmetric conformations with a single pearl and a single string. Thus we conclude that the mobility of charges as an additional degree of freedom brings about interesting conformational behavior.

This work is a part of the research plan of the Faculty of Science of the Charles University, MSM0021620857, supported by the Ministry of Education, Youth and Sports of the Czech Republic. It was further supported by the Grant Agency of the Academy of Sciences of the Czech Republic (Grants KJB401110701 and IAA401110702), Grant Agency of the Charles University (Grant 43-257269), Grant Agency of the Czech Republic (Grants 203/05/H001 and 203/07/0659) and the Marie Curie Research and Training Network (RTN 505027, Polyamphi). The authors would like to thank the METACentrum (CESNET) for the computer time.

REFERENCES

1. Dautzenberg H., Jaeger W., Kötz B. P. J., Seidel C., Stscherbina D.: *Polyelectrolytes: Formation, Characterization and Applications*. Hanser Publishers, Munich 1994.

2. *Polyelectrolytes with Defined Molecular Architecture I* (M. Schmidt, Ed.). *Adv. Polym. Sci.* **2004**, *165*.
3. *Polyelectrolytes with Defined Molecular Architecture II* (M. Schmidt, Ed.). *Adv. Polym. Sci.* **2004**, *166*.
4. Laria D., Wu D., Chandler D.: *J. Chem. Phys.* **1991**, *95*, 4444.
5. Edwards S. F., Singh P. J.: *J. Chem. Soc., Faraday Trans.* **1979**, *275*, 1001.
6. Grest G. S., Kremer K.: *Phys. Rev. A* **1986**, *33*, 3628.
7. Holm C., Kremer K., Deserno M., Limbach H.-J.: *NIC Symposium 2001, Proceedings*, NIC Series (H. Rolnik and D. Wolf, Eds), Vol. 9, p. 385. John von Neumann Institute for Computing, Jülich 2002.
8. Limbach H. J., Holm C.: *J. Chem. Phys.* **2001**, *114*, 9674.
9. Limbach H. J., Holm C.: *J. Phys. Chem.* **2003**, *107*, 8041.
10. Micka U., Holm C., Kremer K.: *Langmuir* **1999**, *15*, 4033.
11. Stevens M., Kremer K.: *Phys. Rev. Lett.* **1993**, *71*, 2228.
12. Khokhlov A. R.: *J. Phys. A* **1980**, *13*, 979.
13. Ghiggino K. P., Roberts A. J., Phillips D.: *Adv. Polym. Sci.* **1981**, *40*, 69.
14. Kantor Y., Kardar M.: *Phys. Rev. E* **1995**, *51*, 1299.
15. Lord Rayleigh: *Philos. Mag.* **1882**, *14*, 184.
16. Dobrynin A. V., Rubinstein M., Obukhov S. P.: *Macromolecules* **1996**, *29*, 2974.
17. Lide D. R. (Ed.): *Handbook of Chemistry and Physics*. CRC Press, New York 1996.
18. Raphael E., Joanny J. F.: *Europhys. Lett.* **1990**, *13*, 623.
19. Ulrich S., Laguecir A., Stoll S.: *J. Phys. Chem.* **2005**, *122*, Art. No. 094911.
20. Uyaver S., Seidel C.: *J. Chem. Phys.* **2004**, *108*, 18804.
21. Borukhov I., Andelman D., Borrega R., Cloitre M., Leibler L., Orland H.: *J. Phys. Chem. B* **2000**, *104*, 11027.
22. Zito T., Seidel C.: *Eur. Phys. J. E* **2002**, *8*, 339.
23. Limbach H.-J., Arnold A., Mann B. A., Holm C.: *Comput. Phys. Commun.* **2006**, *174*, 704.
24. http://www.espresso.mpg.de.
25. Allen M. P., Tildesley D. J.: *Computer Simulation of Liquids*. Clarendon Press, Oxford 1987.
26. Bamford C. H., Tripper C. F. H. (Eds): *Comprehensive Chemical Kinetics*, Vol. 8. Elsevier, Amsterdam 1977.